

EZH2 is involved in psoriasis progression by impairing miR-125a-5p inhibition of SFMBT1 and leading to inhibition of the TGF β /SMAD pathway

Shengming Qu, Zhe Liu and Bing Wang 

Ther Adv Chronic Dis

2021, Vol. 12: 1–15

DOI: 10.1177/
2040622320987348

© The Author(s), 2021.
Article reuse guidelines:
sagepub.com/journals-
permissions

Abstract

Aims: In this study, we aimed to decipher the impact of enhancer of zeste homolog 2 (EZH2) in psoriasis as well as the underlying mechanism.

Methods: A mouse model of psoriasis was developed by means of imiquimod induction, with the expression of EZH2, microRNA-125a-5p (miR-125a-5p), and SFMBT1 determined. The role of EZH2, miR-125a-5p, and SFMBT1 in malignant phenotypes of HaCaT cells and the development of psoriasis *in vivo* was subsequently investigated through gain- and loss-of-function experiments. Chromatin immunoprecipitation assay and dual-luciferase reporter assay were conducted to explore the relationship between EZH2 or SFMBT1 and miR-125a-5p. Finally, the effects of EZH2 and miR-125a-5p on the transforming growth factor β (TGF β)/SMAD pathway were analyzed.

Results: Overexpressed SFMBT1 and EZH2 was detected while miR-125a-5p were downregulated in psoriasis tissues and human keratinocyte (HaCaT) cells. EZH2 increased the levels of IL-17A-induced cytokines and promoted the malignant phenotypes of HaCaT cells. Functionally, EZH2 reduced miR-125a-5p expression while miR-125a-5p targeted SFMBT1 to activate the TGF β /SMAD pathway *in vitro*. Knockdown of EZH2 or up-regulation of miR-125a-5p inhibited cell proliferation and the levels of IL-17A-induced cytokines, but increased the expression of TGF β 1 and the extent of smad2 and smad3 phosphorylation in HaCaT cells. Notably, EZH2 contributed to the development of psoriasis *in vivo* by inhibiting the TGF β /SMAD pathway *via* impairment of miR-125a-5p-mediated SFMBT1 inhibition.

Conclusion: Taken together, the results of the current study highlight the ability of EZH2 to potentially inactivate the TGF β /SMAD pathway *via* upregulation of miR-125a-5p-dependent SFMBT1 during the progression of psoriatic lesions.

Keywords: EZH2, microRNA-125a-5p, SFMBT1, TGF β /SMAD pathway, psoriasis

Received: 17 June 2020; revised manuscript accepted: 21 December 2020.

Introduction

As an immune-mediated chronic inflammatory disease, psoriasis is a debilitating disorder that affects the skin and joints of approximately 2% of the global population.¹ Psoriasis is characterized by an array of symptoms including erythema, epidermal thickening, infiltration, and desquamation, all of which are often used to quantify the

severity of the disease.² Psoriatic keratinocytes can trigger an innate immune response during the early phase of psoriasis development, highlighting the relationship between immune cells and skin-resident keratinocytes in the development of inflammatory and immune responses in psoriasis.³ Interleukin (IL)-17A has been implicated in the proliferation potential of epidermal keratinocytes,

Correspondence to:

Bing Wang

Department of
Dermatology, The Second
Hospital of Jilin University,
No. 218, Ziqiang Road,
Changchun, Jilin Province
130041, P.R. China
wangbing513562@jlu.edu.cn

Shengming Qu
Zhe Liu

Department of
Dermatology, The Second
Hospital of Jilin University,
Changchun, P.R. China

with studies suggesting it plays a vital role in the pathogenesis of numerous immune-mediated diseases including psoriasis.⁴ Therefore, IL-17A in keratinocytes is considered to play a crucial role in establishing and sustaining psoriasis.

From a genetic perspective, the existing literature has emphasized the role of aberrant expression displayed by various genetic factors culminating with inflammation, epidermal proliferation, and immune dysregulation, ultimately leading to the development of psoriasis.⁵ In light of the knowledge that abnormal gene expression has been strongly implicated in epigenetic modifications, a previous study demonstrated the role of aberrant histone modification in the peripheral blood mononuclear cells of *psoriasis vulgaris* patients.⁶ Of note, the enhancer of zeste homolog 2 (EZH2), a histone methyltransferase, has also been shown to participate in various cellular processes such as cancer formation, cellular differentiation, and cellular cycle regulation.⁷ However, the underlying molecular mechanism and its role in psoriasis remain somewhat elusive. Hence, the present study aimed to elucidate the effect of EZH2 on IL-17A-induced cytokine levels and to investigate its related signaling pathways in psoriasis.

Notably, the overexpression of EZH2 has been identified in the abnormal differentiation and disordered growth of epidermal cells in psoriasis.⁸ Nonetheless, being a cellular regulator, EZH2 has been reported to down-regulate the expression of microRNA-125a (miR-125a).⁹ MicroRNAs (miRNAs) represent a class of non-coding RNAs capable of exerting crucial influence in the development of psoriasis.¹⁰ For instance, miR-203 is up-regulated in psoriatic plaques and participates in inflammatory response and keratinocytes by regulating SOCS-3.¹¹ Moreover importantly, it has been documented that miR-125a exhibits significantly reduced expression in psoriasis.¹² Emerging evidence has highlighted the pivotal role played by miRNAs' attributes to the regulatory properties in the expression of their targets.¹³ A study reported there to be a significant elevation in the expression of Scm (Sex comb on midleg) with four MBT (malignant brain tumor) domains 1 (SFMBT1) in psoriasis patients whilst miR-20a-3p has been reported to target SFMBT1, which further inhibits keratinocyte proliferation by regulating the transforming growth factor- β 1 (TGF β 1).¹⁴ TGF β is a member of the TGF β superfamily and is encoded

in mammals by 33 genes involved in control of cell proliferation and differentiation, wound healing, and immune system.¹⁵ TGF β encodes a context-dependent signal which comprises multiple positive and negative modifiers of the essential elements of the receptors, the signaling pathway, and the SMAD proteins.¹⁶ Inactivation of the TGF β /SMAD pathway has been identified to induce keratinocyte proliferation, thus contributing to the pathogenesis of psoriasis.¹⁷ Based on the aforementioned findings, we hypothesized that EZH2 influences keratinocyte proliferation and IL-17A-induced cytokine levels and plays a vital role in the pathogenesis of psoriasis *via* regulation of a potential miR-125a-5p/SFMBT1/TGF β axis. Therefore, we conducted tissue, cell, and animal experiments in this research to verify this hypothesis.

Methods

Ethics statement

The current research was implemented with the ratification of the Clinical Research Ethics Committee of the Second Hospital of Jilin University (No. 201809008) by conforming to the Declaration of Helsinki. All participants signed consent documentation prior to enrollment into the study. All animal experiments were implemented in line with the ratification of the Animal Ethics Committee of the Second Hospital of Jilin University (No. 201907012). Extensive efforts were made to ensure minimal suffering of the included animals.

Bioinformatics analysis

Bioinformatics analysis was conducted through psoriasis-related microarray dataset GSE142582 including gene and miRNA expression data, which were retrieved from the Gene Expression Omnibus database (<https://www.ncbi.nlm.nih.gov/gds>). After differential analysis of the dataset containing five normal samples and five psoriasis samples, the R "edgR" package was employed to screen psoriasis-related differentially expressed genes with $|\log_{2}FC| > 1$ and $p < 0.05$ as the screening criteria.

Clinical tissue collection

Thirty skin biopsies were attained from patients with *psoriasis vulgaris* (18 males and 12 females, aged 26.07 ± 5.10 years), all of whom were yet to

undergo systemic treatment, phototherapy, or the use of topical drugs for at least 3 months. Thirty additional normal skin biopsies were harvested from healthy volunteers (16 males and 14 females, aged 24.47 ± 3.88 years) as controls. All tissues were stored at -80°C for the following experiments.

Cell culture and transfection

Human keratinocyte (HaCaT) incubation was carried out with Dulbecco's modified Eagle's medium (Gibco, Carlsbad, CA, USA) encompassing 10% fetal bovine serum (Gibco), 100 U/mL penicillin, and 100 $\mu\text{g}/\text{mL}$ streptomycin in a humidified environment with 5% CO_2 at 37°C . The cells were subsequently transfected with miR-125a-5p mimic (50 nM), miR-125a-5p mimic negative control (NC) (50 nM), miR-125a-5p inhibitor (100 nM), miR-125a-5p inhibitor NC (100 nM) (RiboBio, Guangdong, China), or short hairpin RNA (sh)-EZH2/NC/SFMBT1/vector (60 nM) (GenePharma, Shanghai, China) respectively using Lipofectamine 2000 reagent as per the manufacturer's directions (Invitrogen, Carlsbad, CA, USA). The sh-RNA sequences for the transfection were as follows: sh-NC: TTCTCCGAACGTGTACGTTT; sh-EZH2-1: CCAACACAA GTCATCCCATTA; sh-EZH2-2: TATGATGG TTAACGGTGATCA. After 24 h of transfection had been performed as described above, the cells were stimulated with IL-17A (100 ng/mL) with the supernatant collected after 12 h. The chemokine level was determined using the MagneticLuminex® Assay multiplex kit (R & D Systems, Minnesota, USA). The Luminex® 200 analyzer was applied to determine the median fluorescence intensity.

Establishment of mouse psoriasis models

Mouse models of psoriasis were developed in BALB/c mice by 3.125 mg of imiquimod (IMQ; 5% Aldara, 3M Pharmaceuticals, Los Angeles, CA, USA) in 62.5 mg lotion/day per 5 cm^2 for six consecutive days. The IMQ-induced mouse models were intra-cutaneously injected with sh-EZH2/sh-NC lentivirus (1×10^9 pfu/100 μL) (GenePharma) for 3 days with the skin samples collected and stored at -80°C . Finally, the clinical score was evaluated by three independent researchers while the scores relating to the degree of erythema, desquamation, and thickness were rated from 0 to 4 (0, none; 1, mild; 2, moderate; 3, severe; 4, very severe).

Reverse transcription-quantitative polymerase chain reaction (RT-qPCR)

Subsequent to 24-h transfection, total RNA extraction from human skin tissues and mouse skin tissues or cells was implemented using the TRIzol reagents (Invitrogen), and the primers used in our study were designed and synthesized by the Invitrogen Company (Table 1). The TaqMan™ MicroRNA RT Kit (4366596, Thermo Fisher Scientific, Waltham, MA, USA) as well as a High-Capacity cDNA RT Kit (4368813, Thermo Fisher Scientific) was employed to synthesize cDNA from the extracted RNA in light of the manufacturer's protocol. RT-qPCR was subsequently operated on the ABI 7500 qPCR instrument (Thermo Fisher Scientific) using the SYBR® Premix Ex Taq™ (Tli RNaseH Plus) kit (RR820A, Takara, Otsu, Shiga, Japan) in accordance with the manufacturer's instructions. Gene expression was evaluated using the $2^{-\Delta\Delta\text{Ct}}$ method and standardized by β -actin and U6.

Western blot analysis

Total protein received extraction using radioimmunoprecipitation assay lysis buffer (R0010, Solarbio, Beijing, China) with the protein concentration determined using a bicinchoninic acid protein assay kit (GBCBIO, Guangdong, China). Subsequent to separation from each sample by 10% sodium dodecyl sulfate-polyacrylamide gel electrophoresis, 40 μg protein was then electroblotted onto a polyvinylidene fluoride membrane (Merck Millipore, Billerica, MA, USA). The membrane was then blocked with Tris-buffered saline Tween encompassing 5% bovine serum albumin at room temperature for 1 h before overnight membrane incubation with primary antibodies (Abcam, Cambridge, UK) against B-cell lymphoma 2 (Bcl-2) (1:1000, ab196495), EZH2 (1:500, ab191080), SFMBT1 (1:2000, ab114863), Ki-67 (1:1000, ab16667), Cyclin D1 (1:200, ab16663), Bcl-2-associated X protein (Bax) (1:1000, ab32503), TGF β 1 (1:1000, ab92486), phosphorylated (p)-smad3 (1:2000, ab52903), p-smad2 (1:1000, ab184557), and glyceraldehyde-3-phosphate dehydrogenase (1:2500, ab9485) at 4°C . The next day, the membrane was re-probed with goat anti-rabbit secondary antibody of immunoglobulin G (IgG; ab97051, 1:2000, Abcam) at ambient temperature. Subsequent to visualization of immune complexes on the membrane with enhanced chemiluminescence reagent, band

Table 1. Primer sequences for reverse transcription-quantitative polymerase chain reaction.

Target	Sequences
EZH2 (human)	Forward: 5'-GATGGGAAAGTACACGGGGA-3' Reverse: 5'-TGCTGTGCCCTTATCTGGAA-3'
SFMBT1 (human)	Forward: 5'-GGAGGAAGGCTGAAGCTACG-3' Reverse: 5'-GTCTAATGGCTGAAGGGGGC-3'
miR-125a-5p (human)	Forward: 5'-GCTCCCTGAGACCCT-3' Reverse: 5'-GAGCAGGCTGGAGAA-3'
β -actin (human)	Forward: 5'-CACGGCTTGCTTACTGAAGG-3' Reverse: 5'-TAATGTCACGCACGATTTCC-3'
U6 (human)	Forward: 5'-CTCGCTTCGGCAGCACA-3' Reverse: 5'-AACGCTTCACGAATTTGCGT-3'
miR-125a-5p (mice)	Forward: 5'-GCGTCCCTGAGACCCTTTAAC-3' Reverse: 5'-AGTGCAGGGTCCGAGGTATT-3'
U6 (mice)	Forward: 5'-GCATGACGTCTGCTTTGGA-3' Reverse: 5'-CCACAATCATTCTGCCATCA-3'
EZH2, enhancer of zeste homolog 2; miR-125a-5p, microRNA-125a-5p; SFMBT1, Scm (Sex comb on midleg) with four MBT (malignant brain tumor) domains 1.	

intensity quantification was conducted using the Image Quant LAS 4000C gel imager (General Electric Company, USA).

Hematoxylin-eosin staining

The mouse skin samples underwent 24-h 4% paraformaldehyde fixing and dehydration before 4- μ m paraffin-embedded serial sections were made. The sections were then dewaxed, and stained with hematoxylin for 5 min, followed by 3-min 5% eosin counterstaining, xylene clearing, sealing, and microscopic observation.

Immunohistochemistry (IHC)

The prepared paraffin sections of skin tissues were heated in a 60°C oven for 30 min, dewaxed, and hydrated in a routine fashion followed by microwave antigen retrieval using 1 mM Tris-ethylenediamine tetraacetic acid (pH = 8.0) as well as endogenous peroxidase blocking with 3% H₂O₂-methanol. The sections were subsequently incubated with primary antibodies against EZH2

(1:250, ab191080, Abcam), IL-17A (1:600, ab214588, Abcam), Ki-67 (1:200, ab16667, Abcam), or SFMBT1 (1:1000, HPA036153, Sigma-Aldrich, St. Louis, MO, USA) in a 4°C refrigerator overnight. The next day, the sections were probed with polymer enhancer (PV-9000, ZSGB-Bio, Beijing, China) at ambient temperature for 20 min. The sections were incubated with enzyme-labeled anti-rat/rabbit polymer (PV-9000, ZSGB-Bio) at ambient temperature for 30 min and visualized with 3,3'-diaminobenzidine tetrahydrochloride for 5 min. The sections were then counterstained with hematoxylin, followed by the addition of ammonium hydroxide. Finally, the sections were routinely dehydrated, cleared, and sealed followed by observation and photograph under an inverted microscope (CX41, Olympus Optical Co., Ltd, Tokyo, Japan).

Dual-luciferase reporter assay

The Targetscan database was used to predict target genes of miR-125a-5p and dual-luciferase reporter gene assay was performed to verify whether

SFMBT1 is a direct target of miR-125a-5p. For this purpose, fragments of human or rat SFMBT1 wild type (WT) 3' untranslated region (UTR) and its complementary sequence mutant type (MUT) sites were artificially synthesized and cloned into pMIR-reporter (Beijing Huayueyang Biotechnology Co., Ltd, Beijing, China) using endonuclease sites SpeI and Hind III. The correctly sequenced WT or MUT luciferase reporter plasmids were co-transfected with human/rat miR-125a-5p mimic and NC-mimic into HEK293T cells (Shanghai Beinuo Biotechnology Co., Ltd, Shanghai, China). After a 48 h period of transfection, luciferase activity was determined using the dual-luciferase reporter assay system (Promega, Madison, Wisconsin, USA) with the Glomax 20/20 luminometer (Promega). The relative luciferase activity was calculated based on the activity of firefly luciferase/activity of renilla luciferase.

Chromatin immunoprecipitation assay (ChIP)

The 70–80% confluent cells were fixed with 1% formaldehyde at room temperature for 10 min to crosslink. The crosslinked DNA and protein were sonicated into fragments followed *via* centrifugation at 10,000 *g* at 4°C for supernatant collection purposes. Half of the supernatant was added with anti-rabbit antibody against IgG (ab109489, 1:100, Abcam) while the other half was added with anti-rabbit antibody against EZH2 (ab191250, 1:100, Abcam) for overnight incubation at 4°C. Then, the endogenous DNA–protein complex was immunoprecipitated using Protein Agarose/Sepharose followed by centrifugation which allowed for removal of the supernatant after which the non-specific complex was washed and de-crosslinked overnight at 65°C. Finally, DNA fragments were extracted and purified using the phenol/chloroform. Finally, the qPCR analysis was used to verify the enrichment of EZH2 in the promoter region of miR-125a-5p.

Flow cytometry

Subsequent to 48-h transfection, the cells were attained and resuspended to a density of approximately 1×10^6 /mL and 0.5 mL of the cell suspension (5×10^5 cells) was transferred into a clean centrifuge tube followed by the addition of the staining fluid. Next, the cells were resuspended with 0.5 mL of pre-chilled $1 \times$ binding buffer and stained with 5 μ L of Annexin V-fluorescein isothiocyanate and 10 μ L of propidium iodide. After

15 min of incubation under conditions void of light, a flow cytometer (FACSVerse/Calibur/AriaIIISORP, BD Biosciences, San Jose, CA, USA) was employed to identify and analyze cell apoptosis. The aforementioned reagents were purchased from Beyotime (Shanghai, China).

5-ethynyl-2'-deoxyuridine (EdU) assay

The cells were fixed in 4% paraformaldehyde and stained with Apollo567 followed by Hoechst 33342 (Cell-light Edu Kit, Ribobio). A FV-1000/ES confocal microscope was used for image capture.

Statistical analysis

All data were processed using SPSS 21.0 statistical software (IBM Corp., Armonk, NY, USA). Measurement data were expressed as the mean \pm standard deviation. Data between two groups were compared by independent sample *t*-test while data between multiple groups were compared by one-way analysis of variance and Tukey's post hoc test. Pearson's correlation analysis was applied to analyze the correlation between miR-125-5p expression and SFMBT1 expression. Statistical significance was reflected by $p < 0.05$.

Results

Highly expressed EZH2 in clinical tissue samples of psoriasis patients

The existing literature has previously demonstrated the overexpression of EZH2 in psoriasis.⁸ Our data obtained from psoriasis-related microarray GSE142582 also confirmed an elevated expression of EZH2 (Figure 1A). Moreover, the RT-qPCR and Western blot analyses revealed a significantly increased expression of EZH2 in the psoriatic skin tissues (Figure 1B–D). Meanwhile, IHC results further confirmed that the distribution of EZH2 was markedly increased in the psoriatic skin tissues (Figure 1E). Altogether, the aforementioned data provided evidence attesting the notion that EZH2 is overexpressed in psoriasis.

Knockdown of EZH2 inhibited keratinocyte proliferation and decreased IL-17A induced cytokine levels

Next, to further elucidate the role of EZH2 in psoriasis, EZH2 was knocked down in HaCaT

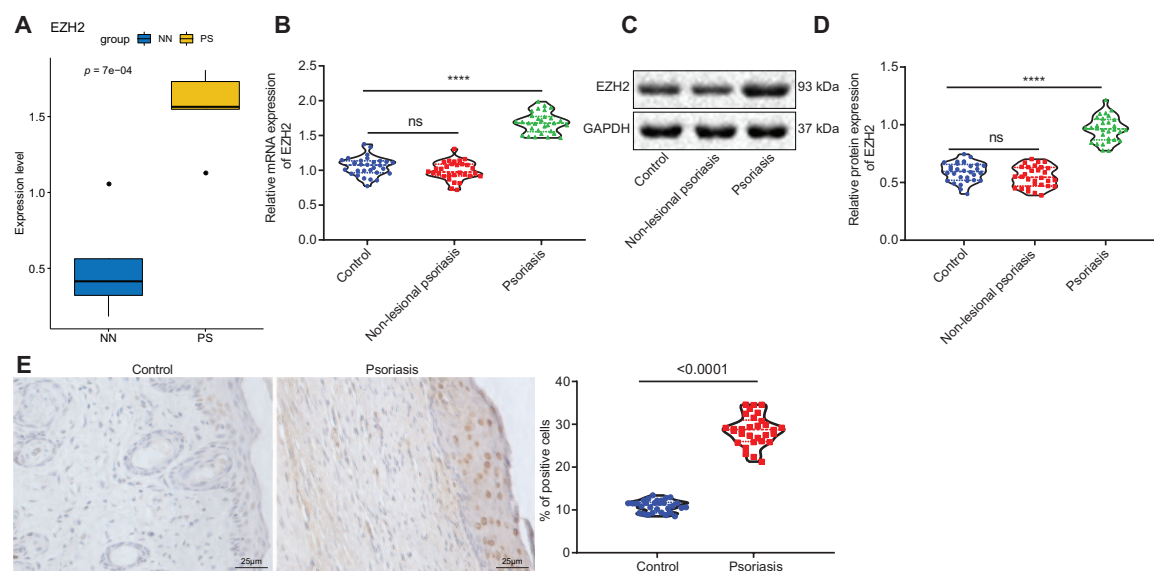


Figure 1. EZH2 was highly expressed in psoriasis. (A) Expression of EZH2 in the microarray database (NN on the horizontal axis represents normal skin tissues and PS represents psoriatic skin tissues). (B) Reverse transcription-quantitative polymerase chain reaction determination of the EZH2 expression in psoriatic skin tissues and normal skin tissues in non-lesional skin and lesional skin tissues. (C) Western blot analysis of the EZH2 expression in psoriatic skin tissues and normal skin tissues in non-lesional skin and lesional skin tissues normalized to GAPDH. (D) Quantitation of panel C. (E) Immunohistochemistry detection of the EZH2 expression in psoriatic skin tissues and normal skin tissues ($\times 400$). The results of the data were measurement data, which were presented as the mean \pm standard deviation and analyzed by independent-sample *t*-test, $N=30$. EZH2, enhancer of zeste homolog 2; GAPDH, glyceraldehyde-3-phosphate dehydrogenase; mRNA, messenger RNA.

cells. RT-qPCR and Western blot analysis results demonstrated that transfection with sh-EZH2-1 and sh-EZH2-2 markedly inhibited the expression of EZH2, of which sh-EZH2-1 resulted in a more pronounced effect (Figure 2A and B) and was thus selected for subsequent experiments. Moreover, the results of EdU assay and flow cytometry indicated that the silencing of EZH2 significantly inhibited the proliferation of HaCaT cells but a significantly increased apoptosis was observed (Figure 2C and D). Western blot analysis provided further verification that the depletion of EZH2 noticeably reduced the expression of proliferation- and apoptosis-related proteins (Ki-67, Cyclin D1, and Bcl-2) while acting to upregulate the expression of Bax (Figure 2E).

Also, the involvement of IL-17A has been previously documented in the regulation of pro-inflammatory chemokines with studies highlighting its important role in the pathophysiology of immune-mediated diseases such as psoriasis.⁴ Consistently, our results indicated that after treating HaCaT

cells with IL-17A, the levels of cytokines CCL2, CCL7, CCL20, CXCL1, CXCL2, CXCL5, CXCL8, and CXCL10 were markedly increased (Figure 2F). However, following knockdown of EZH2, the levels of the above-described cytokines in IL-17A-treated HaCaT cells were significantly decreased (Figure 2G). Collectively, the aforementioned results provided evidence demonstrating that knockdown of EZH2 inhibited the keratinocyte proliferation as well as the levels of IL-17A-induced cytokines.

Down-regulation of EZH2 hindered keratinocyte proliferation and decreased IL-17A induced cytokine levels by enhancing miR-125a-5p

A previous work revealed poor expression of miR-125a-5p in psoriatic skin tissues.¹⁰ EZH2 is enriched in the miR-125a-5p promoter region which leads to the inhibition of miR-125a-5p expression.⁹ Our RT-qPCR results demonstrated that the knockdown of EZH2 in HaCaT cells significantly increased the expression of

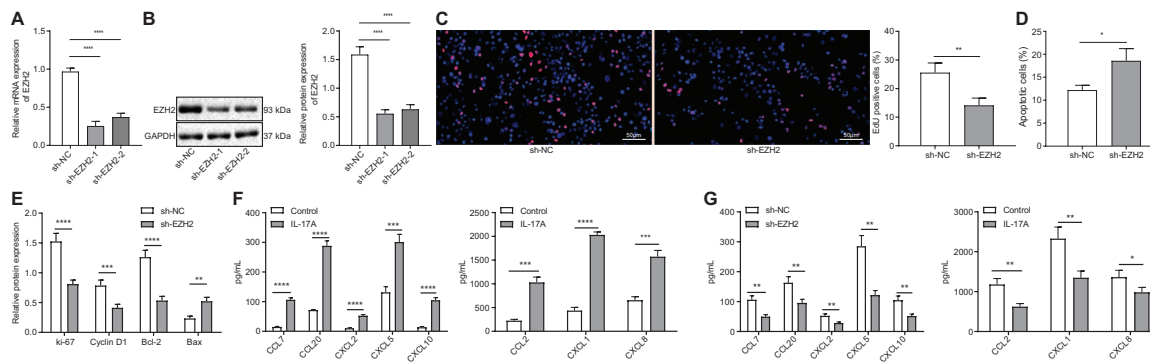


Figure 2. Down-regulation of EZH2 suppressed keratinocyte proliferation and IL-17A-induced cytokine levels. (A) Reverse transcription-quantitative polymerase chain reaction determination of EZH2 expression in human keratinocyte (HaCaT) cells after sh-EZH2-1 and sh-EZH2-2 treatment. (B) Western blot analysis of the EZH2 expression in HaCaT cells after sh-EZH2-1 and sh-EZH2-2 treatment normalized to GAPDH. (C) EdU detection of HaCaT cell proliferation after sh-EZH2 treatment ($\times 200$). (D) HaCaT cell apoptosis after sh-EZH2 treatment assessed by flow cytometry. (E) Western blot analysis of the expression of Ki-67, Cyclin D1, Bcl-2, and Bax in HaCaT cells after sh-EZH2 treatment normalized to GAPDH. (F) CCL2, CCL7, CCL20, CXCL1, CXCL2, CXCL5, CXCL8, and CXCL10 levels in HaCaT cells induced by IL-17A. G, CCL2, CCL7, CCL20, CXCL1, CXCL2, CXCL5, CXCL8, and CXCL10 levels in HaCaT cells after EZH2 knockdown. In panels A–G, $*p < 0.05$ compared with treatment of sh-NC, and in panel F, $*p < 0.05$ compared with control. The results of the data were measurement data, which were presented as the mean \pm standard deviation and analyzed by independent-sample *t*-test. Also, data between multiple groups were compared with one-way analysis of variance. * ** and **** indicate comparison between the two groups. EdU, 5-ethynyl-2'-deoxyuridine; EZH2, enhancer of zeste homolog 2; sh, short hairpin RNA; GAPDH, glyceraldehyde-3-phosphate dehydrogenase; NC, negative control; mRNA, messenger RNA.

miR-125a-5p (Figure 3A). The ChIP results illustrated that EZH2 was enriched in the miR-125a-5p promoter region in HaCaT cells. However, after EZH2 was knocked down, the enrichment of EZH2 in the miR-125a-5p promoter region was markedly suppressed (Figure 3B). Moreover, the microarray dataset GSE142582 also exhibited a downward trend in the expression of miR-125a-5p in psoriasis (Figure 3C). Intriguingly, RT-qPCR analysis of the miR-125a-5p expression also confirmed the significant reduction in the expression of miR-125a-5p in psoriatic skin tissues (Figure 3D). Furthermore, RT-qPCR and Western blot analysis revealed that reduction of EZH2 triggered a significant increase in the expression of miR-125a-5p while down-regulation of miR-125a-5p did not exhibit any significant effect on EZH2 expression (Figure 3E and F), suggesting that miR-125a-5p could be downstream of EZH2.

Furthermore, the EdU and flow cytometry results revealed that miR-125a-5p up-regulation or EZH2 knockdown remarkably inhibited the proliferation of HaCaT cells but an increase in apoptosis was observed, which could be reversed by

the down-regulation of miR-125a-5p (Figure 3G and H). Western blot analysis revealed that over-expression of miR-125a-5p or silencing of EZH2 led to a distinct reduction in the expression of Ki-67, Cyclin D1, and Bcl-2 but enhanced that of Bax in HaCaT cells. However, these changes were reversed *via* the downregulation of miR-125a-5p (Figure 3I). Additionally, the overexpression of miR-125a-5p or knockdown of EZH2 significantly decreased the expression of CCL2, CCL7, CCL20, CXCL1, CXCL2, CXCL5, CXCL8, and CXCL10 after IL-17A treatment, which could also be reversed by the down-regulation of miR-125a-5p (Figure 3J). The aforementioned results indicated that down-regulation of EZH2 inhibited keratinocyte proliferation while decreasing IL-17A induced cytokine levels by increasing the expression of miR-125a-5p.

EZH2 up-regulated the expression of the miR-125a-5p target SFMBT1

The Targetscan website predicted the presence of binding sites between miR-125a-5p and SFMBT1 (Figure 4A). Additionally, the luciferase reporter assay results confirmed interactions by exhibiting

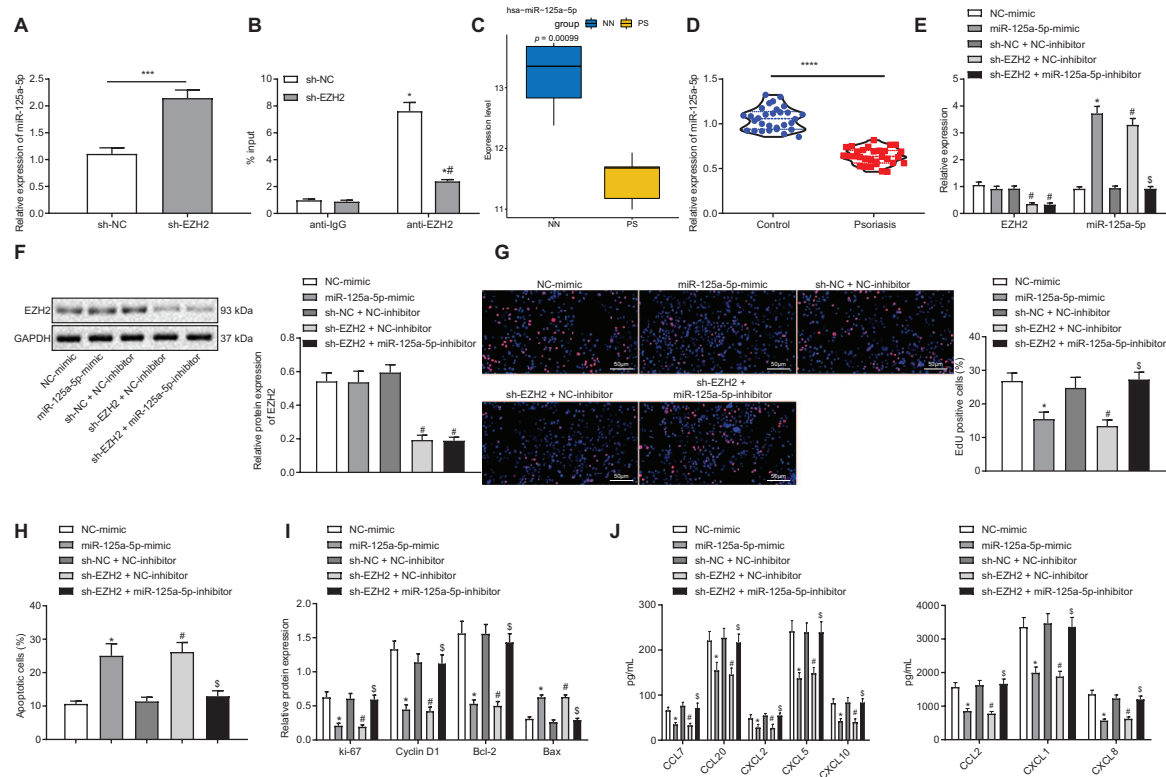


Figure 3. Down-regulation of EZH2 increased the expression of miR-125a-5p to impede the proliferation of keratinocytes and decreased IL-17A-induced cytokine levels. (A) Reverse transcription-quantitative polymerase chain reaction (RT-qPCR) determination of the expression of miR-125a-5p in human keratinocyte (HaCaT) cells after sh-EZH2 treatment, $*p < 0.05$ compared with the treatment of sh-NC, $***p < 0.001$. (B) ChIP results of EZH2 enrichment in the miR-125a-5p promoter region in HaCaT cells after sh-EZH2 treatment, $*p < 0.05$ compared with treatment of anti-IgG, and $\#p < 0.05$ compared with treatment of anti-EZH2. (C) Expression of hsa-miR-125a-5p in the microarray database (NN in the abscissa indicates normal skin tissue and PS indicates psoriatic skin tissue). (D) RT-qPCR determination of the miR-125a-5p expression in psoriatic skin tissues and normal skin tissues, $*p < 0.05$ compared with normal skin tissues, $****p < 0.0001$. (E) RT-qPCR determination of the EZH2 and miR-125a-5p expression in HaCaT cells after miR-125a-5p mimic, sh-EZH2, or miR-125a-5p inhibitor treatment. (F) Western blot analysis of the EZH2 expression in HaCaT cells after miR-125a-5p mimic, sh-EZH2, or miR-125a-5p inhibitor treatment normalized to GAPDH. (G) EdU assay of HaCaT cell proliferation after miR-125a-5p mimic, sh-EZH2, or miR-125a-5p inhibitor treatment ($\times 200$). (H) HaCaT cell apoptosis after miR-125a-5p mimic, sh-EZH2, or miR-125a-5p inhibitor treatment assessed by flow cytometry. (I) Western blot analysis of the expression of Ki-67, Cyclin D1, Bcl-2, and Bax in HaCaT cells after miR-125a-5p mimic, sh-EZH2, or miR-125a-5p inhibitor treatment normalized to GAPDH. (J) Cytokine levels in HaCaT cells after miR-125a-5p mimic, sh-EZH2, or miR-125a-5p inhibitor treatment. In panels D–I, $*p < 0.05$ compared with treatment of NC-mimic, $\#p < 0.05$ compared with treatment of sh-NC + NC-inhibitor, and $\$p < 0.05$ compared with treatment of sh-EZH2 + NC-inhibitor. The results of the data were measurement data, which were presented as the mean \pm standard deviation and analyzed by independent-sample *t*-test. Also, data between multiple groups were compared with one-way analysis of variance. EdU, 5-ethynyl-2'-deoxyuridine; EZH2, enhancer of zeste homolog 2; sh, short hairpin RNA; GAPDH, glyceraldehyde-3-phosphate dehydrogenase; miR-125a-5p, microRNA-125a-5p; NC, negative control; sh, short hairpin RNA.

(Figure 4B) that the luciferase activity of the WT-SFMBT1 was significantly decreased while that of MUT-SFMBT1 exhibited no significant difference following transfection with miR-125a-5p mimic. Furthermore, RT-qPCR and Western blot analysis demonstrated the remarkably increased expression of SFMBT1 and EZH2

in psoriatic skin tissues (Figure 4C and D). Also, IHC results revealed that the distribution of SFMBT1 expression was markedly increased in psoriatic skin tissues (Figure 4E and F) while miR-125a-5p was identified to be negatively correlated with SFMBT1 expression in clinical skin tissue samples of psoriasis (Figure 4G). RT-qPCR and

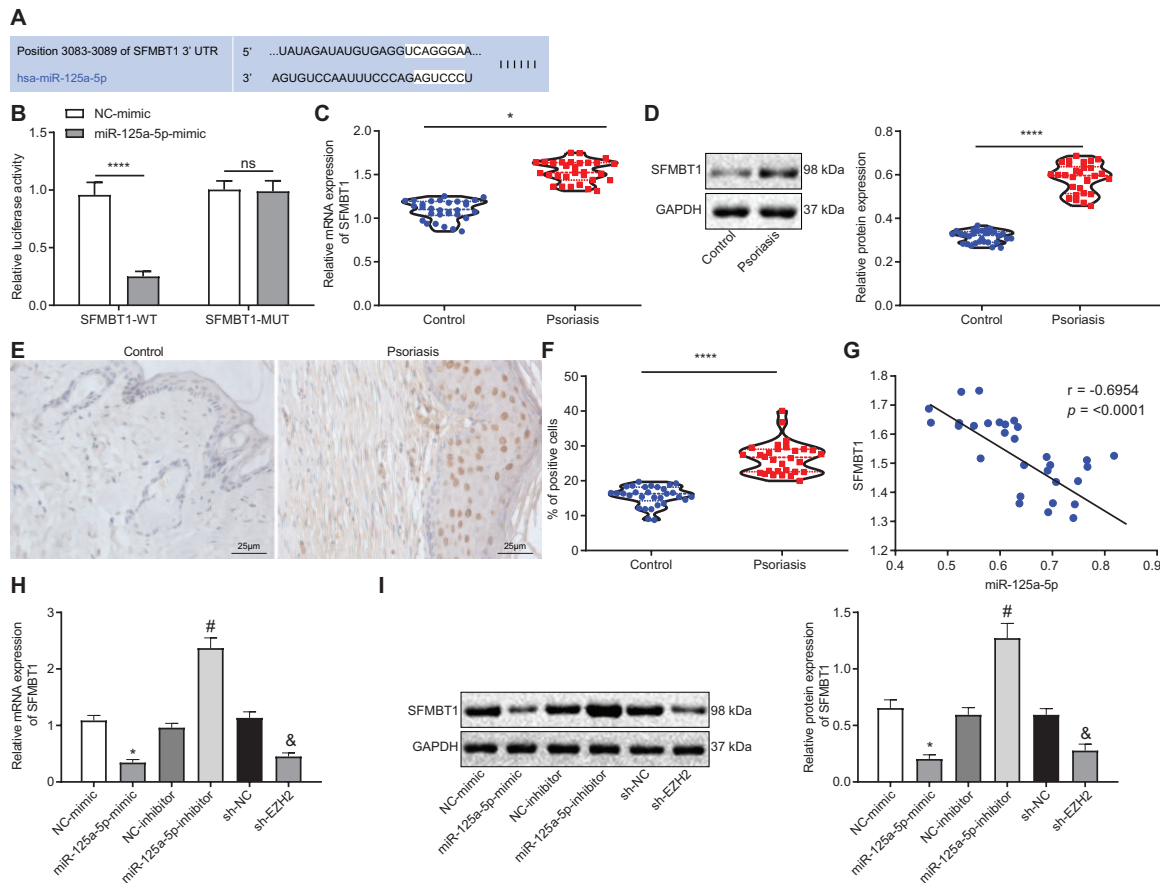


Figure 4. EZH2 inhibited the expression of miR-125a-5p to up-regulate SFMBT1 expression. (A) Binding sites between miR-125a-5p and SFMBT1 predicted through the Targetscan database. (B) Dual-luciferase reporter assay results of interaction between miR-125a-5p and SFMBT1, **** $p < 0.0001$ compared with the treatment of wild-type NC. (C) Reverse transcription-quantitative polymerase chain reaction (RT-qPCR) determination of SFMBT1 expression in psoriatic skin tissues and controls, * $p < 0.05$ compared with control, $N = 30$. (D) Western blot analysis of SFMBT1 expression in psoriatic skin tissues and controls normalized to GAPDH, **** $p < 0.0001$ compared with control, $N = 30$. (E) Immunohistochemistry of SFMBT1 expression in psoriatic skin tissues and controls ($\times 400$). (F) Quantitation of panel E. **** $p < 0.0001$ compared with control, $N = 30$. (G) Correlation analysis between miR-125a-5p expression and SFMBT1 expression in clinical skin tissue samples of psoriasis. (H) RT-qPCR determination of SFMBT1 expression in human keratinocyte (HaCaT) cells after miR-125a-5p-mimic, miR-125a-5p-inhibitor, or sh-EZH2 treatment, * $p < 0.05$ compared with treatment of NC-mimic, # $p < 0.05$ compared with treatment of NC-inhibitor, and & $p < 0.05$ compared with treatment of sh-NC. (I) Western blot analysis of SFMBT1 expression in HaCaT cells after miR-125a-5p-mimic, miR-125a-5p-inhibitor, or sh-EZH2 treatment normalized to GAPDH, * $p < 0.05$ compared with treatment of NC-mimic, # $p < 0.05$ compared with treatment of NC-inhibitor, and & $p < 0.05$ compared with treatment of sh-NC. The data were measurement data, which were presented as the mean \pm standard deviation. Data between the two groups were compared using an independent-sample *t*-test while data between multiple groups were compared using one-way analysis of variance. Pearson's analysis was used to determine the correlation between miR-125a-5p and SFMBT1.

EZH2, enhancer of zeste homolog 2; GAPDH, glyceraldehyde-3-phosphate dehydrogenase; miR-125a-5p, microRNA-125a-5p; MUT, mutant type; NC, negative control; SFMBT1, Scm (Sex comb on midleg) with four MBT (malignant brain tumor) domains 1; sh, short hairpin RNA; WT, wild type; mRNA, messenger RNA.

Western blot analysis results demonstrated that overexpression of miR-125a-5p or knockdown of EZH2 in HaCaT cells triggered a significant decrease in the expression of SFMBT1, whereas

depletion of miR-125a-5p led to a significant increase in the expression of SFMBT1 (Figure 4H and I). Taken together, the aforementioned results revealed that EZH2 up-regulated the expression of

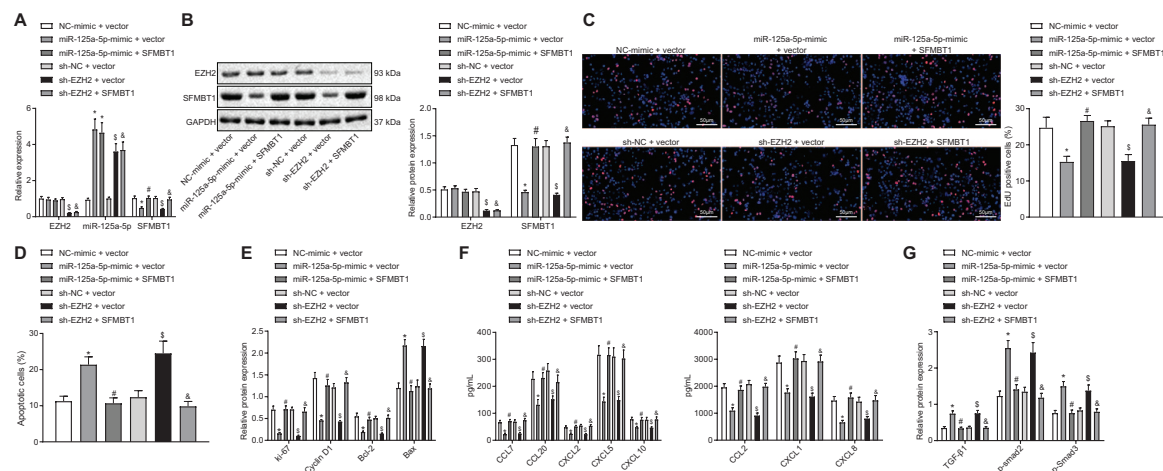


Figure 5. EZH2 inactivated the TGFβ/SMAD pathway by regulating the expression of miR-125a-5p-mediated SFMBT1 to promote keratinocyte proliferation and increase IL-17A-induced cytokine levels. (A) Reverse transcription-quantitative polymerase chain reaction determination of the expression of EZH2, miR-125a-5p, and SFMBT1 in human keratinocyte (HaCaT) cells after miR-125a-5p-mimic, SFMBT1, or sh-EZH2 treatment. (B) Western blot analysis of the EZH2 and SFMBT1 expression in HaCaT cells after miR-125a-5p-mimic, oe-SFMBT1, or sh-EZH2 treatment, normalized to GAPDH. (C) HaCaT cell proliferation assessed by EdU assay after miR-125a-5p-mimic, SFMBT1, or sh-EZH2 treatment (×200). (D) HaCaT cell apoptosis assessed by flow cytometry after miR-125a-5p-mimic, SFMBT1, or sh-EZH2 treatment. (E) Western blot analysis of the Ki-67, Cyclin D1, Bcl-2, and Bax expression in HaCaT cells after miR-125a-5p-mimic, SFMBT1, or sh-EZH2 treatment, normalized to GAPDH. (F) Levels of cytokines CCL2, CCL7, CCL20, CXCL1, CXCL2, CXCL5, CXCL8, and CXCL10 in HaCaT cells after miR-125a-5p-mimic, SFMBT1, or sh-EZH2 treatment. (G) Western blot analysis of the expression of TGFβ1, and the extent of smad2 and smad3 phosphorylation in HaCaT cells after miR-125a-5p-mimic, SFMBT1, or sh-EZH2 treatment, normalized to GAPDH. **p* < 0.05 compared with treatment of NC-mimic + vector, #*p* < 0.05 compared with treatment of miR-125a-5p-mimic + vector, \$*p* < 0.05 compared with treatment of sh-NC + vector, and &*p* < 0.05 compared with treatment of sh-EZH2 + vector. The results of the data were measurement data and presented as the mean ± standard deviation. Data between multiple groups were compared using one-way analysis of variance.

EZH2, enhancer of zeste homolog 2; GAPDH, glyceraldehyde-3-phosphate dehydrogenase; miR-125a-5p, microRNA-125a-5p; NC, negative control; SFMBT1, Scm (Sex comb on midleg) with four MBT (malignant brain tumor) domains 1; sh, short hairpin RNA; TGFβ, transforming growth factor-β.

SFMBT1 by inhibiting the miR-125a-5p expression.

EZH2 inhibited the TGFβ/SMAD pathway to promote keratinocyte proliferation and increase IL-17A-induced cytokine levels by upregulating the expression of miR-125a-5p target SFMBT1

We subsequently set out to investigate the role of the EZH2/miR-125a-5p/SFMBT1 axis in psoriasis. The results of RT-qPCR and Western blot analysis revealed that the overexpression of miR-125a-5p significantly impeded the expression of SFMBT1, which was reversed by the up-regulation of SFMBT. Moreover, the down-regulation of EZH2 noticeably enhanced the miR-125a-5p expression but decreased the expression of SFMBT1, which also could be rescued by

overexpression of SFMBT1 (Figure 5A and B). These results suggested the sequential regulation order among EZH2/miR-125a-5p/SFMBT1.

Also, the results of EdU assay and flow cytometry revealed that overexpression of miR-125a-5p or knockdown of EZH2 noticeably reduced cell proliferation but promoted cell apoptosis, which could be recovered by up-regulation of SFMBT (Figure 5C and D). Moreover, Western blot analysis revealed that miR-125a-5p up-regulation or down-regulation of EZH2 markedly reduced the expression of Ki-67, Cyclin D1, and Bcl-2 in HaCaT cells but increased Bax expression, which could also be reversed by overexpression of SFMBT expression (Figure 5E). Moreover, the up-regulation of miR-125a-5p or down-regulation of EZH2 led to a marked decrease in the

expression of the cytokines CCL2, CCL7, CCL20, CXCL1, CXCL2, CXCL5, CXCL8, and CXCL10 in HaCaT cells after IL-17A treatment, which was reversed *via* enhancement of the SFMBT1 expression (Figure 5F).

SFMBT1 has been reported to promote psoriasis by means of inhibiting the TGF β /SMAD pathway.¹⁴ However, in psoriasis, the TGF β /SMAD pathway has been suggested to be inhibited while its activation results in inhibition of psoriasis.¹⁷ Western blot analysis highlighted that the elevated expression of miR-125a-5p or down-regulation of EZH2 significantly increased the levels of TGF β 1, and the extent of smad2 and smad3 phosphorylation, which could be rescued by overexpression of SFMBT1 (Figure 5G). Thus, based on the aforementioned results, we concluded that EZH2 inhibited the TGF β /SMAD pathway by regulating the expression of miR-125a-5p-dependent SFMBT1, ultimately promoting keratinocyte proliferation and increasing IL-17A-induced cytokine levels.

Knockdown of EZH2 in vivo activated the TGF β /SMAD pathway through modulating the miR-125a-5p-dependent SFMBT1 expression, thereby inhibiting psoriasis

IMQ was applied to trigger skin inflammation in mice in order to establish psoriasis mouse models. In order to verify the effect of EZH2 on psoriasis *in vivo*, sh-NC/sh-EZH2 lentivirus was injected intradermally into the shaved dorsal skin of mice for three consecutive days.

After IMQ treatment, the psoriasis severity score was significantly increased, characterized by a notable increase in epidermal thickness, a large number of infiltrated inflammatory cells, and exacerbated erythema. On the other hand, the silencing of EZH2 noticeably relieved the above manifestations and reduced the psoriasis severity score in modeled mice (Figure 6A). Following IMQ treatment, the expression of miR-125a-5p was notably reduced, which was recovered by depleting the EZH2 expression (Figure 6B). Moreover, our results from Western blot analysis further confirmed that IMQ treatment significantly enhanced the levels of EZH2, SFMBT1, Ki-67, Cyclin D1, and Bcl-2 but the expression of TGF β 1 and the extent of smad2 and smad3 phosphorylation were found to be reduced, a finding of which could be reversed by knockdown of EZH2 (Figure 6C). Furthermore, the IHC results

demonstrated that the Ki-67-, IL-17A-, and EZH2-positive cells in the skin tissues of mice were significantly increased following IMQ treatment, which could also be rescued by down-regulation of EZH2 (Figure 6D). Taken together, our results provided evidence indicating that the knockdown of EZH2 could activate the TGF β /SMAD pathway through regulation of miR-125a-5p-mediated SFMBT1 *in vivo*, which ultimately alleviated epidermal hyperplasia and psoriatic skin inflammation.

Discussion

Sustained inflammation is widely considered to be the hallmark of psoriasis, which consequently leads to unregulated keratinocyte proliferation and dysfunctional differentiation.¹⁸ Recently reported genetic and epigenetic phenomena, including genetic regulation of psoriasis by aberrant histone modification, have been indicated as major causative factors in psoriasis.¹⁹ However, the translation of these findings into clinical therapy remains a major stumbling block from an epigenetic research point of view in psoriasis. Thus it is necessary to generate novel hypotheses to determine the correlation between these factors and the progression of psoriasis. Accordingly, the major objective of the present study was to evaluate the role of histone methyltransferase EZH2 in IL-17A-induced keratinocytes in psoriasis. Key observations made during the current study demonstrated that EZH2 possesses the potential to inhibit the TGF β 1/SMAD pathway, resulting in the stimulation of keratinocyte proliferation and inflammatory reactions, thereby exacerbating psoriasis, through regulation of miR-125a-5p-dependent SFMBT1 (Figure 7).

Initially, we detected considerably higher EZH2 expression in psoriasis tissues which further promoted the keratinocyte proliferation and increased the IL-17A-induced cytokine levels. Further exploration during our study yielded findings indicating that EZH2 significantly increased the expression of Ki-67, Cyclin D1, and Bcl-2, and elevated the levels of IL-17A-induced cytokines such as CCL2, CCL7, CCL20, CXCL1, CXCL2, and CXCL10. Similarly, previous studies have revealed notably enhanced expression of EZH2 in psoriatic skin tissues.^{6,8} The inhibition of EZH2 has also been noted in the existing literature to decrease the expression of keratinocyte chemokines including CCL2, CCL4, CCL5, and CXCL1 *in vivo*, which was partially consistent with our results.²⁰ Besides, the critical involvement of IL-17A and

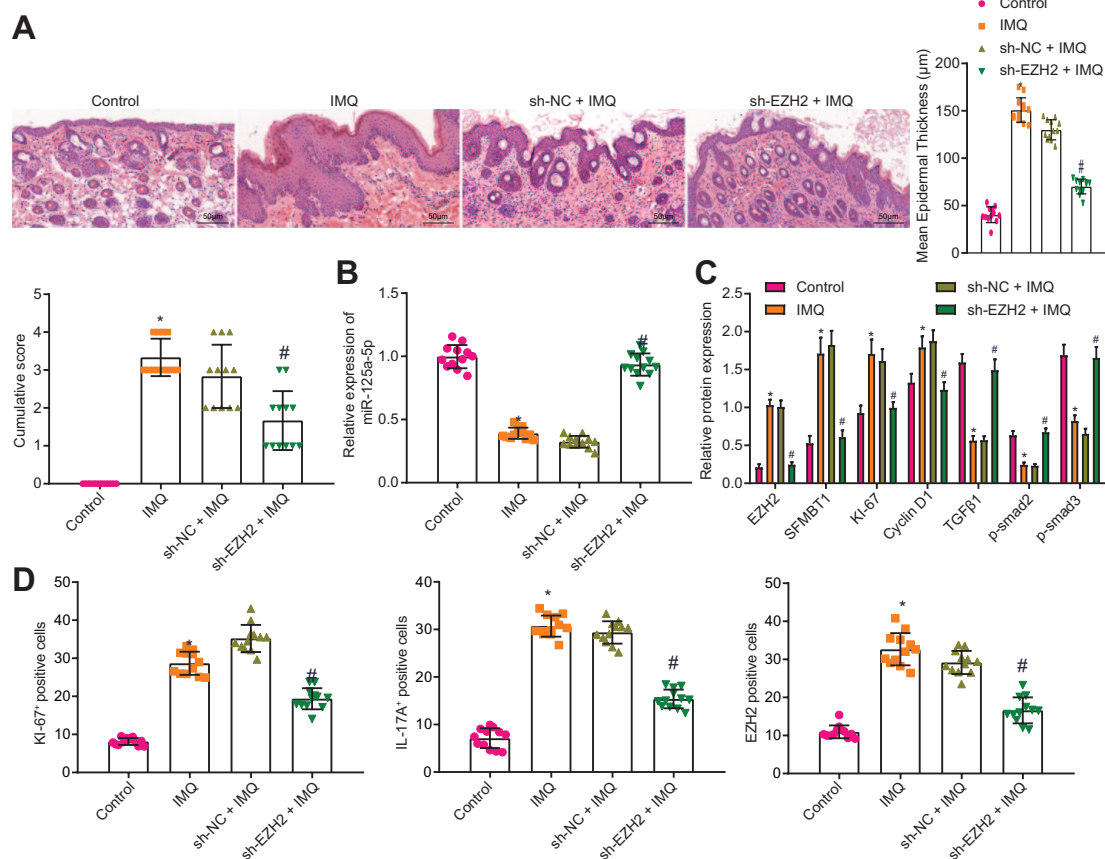


Figure 6. Knockdown of EZH2 *in vivo* activated the TGFβ/SMAD pathway through regulation of miR-125a-5p-mediated SFMBT1 to inhibit psoriasis. (A) Representative macroscopic images of dorsal skin samples and hematoxylin-eosin (HE) staining of skin sections obtained from mice on the fifth day from the start of lentiviral injection, and the cumulative score of epidermal thickness, and erythema of HE-stained skin sections of mice after IMQ induction or IMQ-induced mice with sh-EZH2 treatment was quantified ($\times 200$), $N=8$. (B) Reverse transcription-quantitative polymerase chain reaction determination of the miR-125a-5p expression in skin tissues of mice after IMQ induction or IMQ-induced mice with sh-EZH2 treatment. (C) Western blot analysis of the expression of EZH2, SFMBT1, Ki-67, Cyclin D1, Bcl-2, and TGFβ1, along with the extent of smad2 and smad3 phosphorylation in skin tissues of mice after IMQ induction or IMQ-induced mice with sh-EZH2 treatment normalized to GAPDH. (D) Immunohistochemistry measurement of Ki-67, IL-17A and EZH2 expression in skin tissues of mice after IMQ induction or IMQ-induced mice with sh-EZH2 treatment. * $p < 0.05$ compared with control, # $p < 0.05$ compared with IMQ-induced mice with sh-NC treatment. The results of the data were measurement data and presented by the mean \pm standard deviation. Data between multiple groups were compared using one-way analysis of variance. EZH2, enhancer of zeste homolog 2; GAPDH, glyceraldehyde-3-phosphate dehydrogenase; IMQ, imiquimod; miR-125a-5p, microRNA-125a-5p; NC, negative control; p, phosphorylated; SFMBT1, Scm [Sex comb on midleg] with four MBT [malignant brain tumor] domains 1; sh, short hairpin RNA; TGFβ, transforming growth factor-β.

keratinocytes in the development of psoriasis has also been previously proposed.⁴ Thus, it is reasonable to suggest based on the aforementioned findings that EZH2 could promote keratinocyte proliferation and increase IL-17A-induced cytokine levels to affect psoriasis.

miRNAs continue to be widely investigated as novel biomarkers for diagnosis, to determine the disease severity, and to monitor therapy response. Therefore,

targeting specific miRNAs represents a potentially powerful tool which may prove to be useful in the development of novel therapeutic methods for psoriasis.^{21,22} For example, miR-210 upregulation promoted psoriasis-like inflammation by augmenting Th1 and Th17 cell differentiation.²³ In addition, miR-146a could suppress skin inflammation in psoriasis.^{24–26} Also, miR-125b was downregulated in psoriasis, and its upregulation caused suppression of keratinocyte proliferation by targeting FGFR2.²⁷

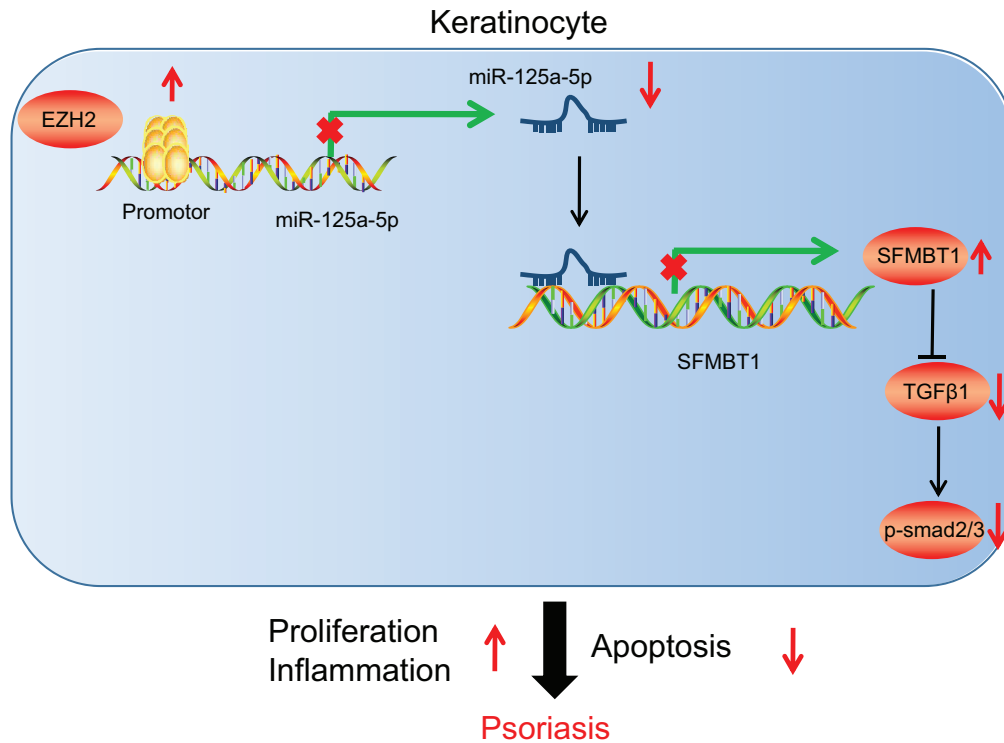


Figure 7. Schematic diagram of the proposed mechanism. EZH2 is enriched in the miR-125a-5p promoter and inhibits miR-125a-5p expression, thereby increasing the expression of the miR-125a-5p target SFMBT1. SFMBT1 further inhibits the expression of TGF β 1, and the extent of smad2 and smad3 phosphorylation (p-smad2/3), and consequently impedes keratinocyte apoptosis and promotes keratinocyte proliferation as well as the inflammatory reactions, eventually exacerbating psoriasis. EZH2, enhancer of zeste homolog 2; miR-125a-5p, microRNA-125a-5p; SFMBT1, Scm (Sex comb on midleg) with four MBT (malignant brain tumor) domains 1; TGF β , transforming growth factor- β .

Additionally, another study also elucidated the involvement of miR-125a in psoriasis.²⁸ Importantly, miR-125a-5p has been reported to suppress cell proliferation and invasion,²⁹ suggesting the role of miR-125a-5p as an inhibitor of abnormal cell growth. Moreover, a further study indicated the enrichment of EZH2 on the promoter region of miR-125a, which illustrates EZH2 as a contributor to low expression of miR-125a.⁹ Consistently, our findings revealed that EZH2 inhibited the expression of miR-125a-5p in skin cells.

A key finding of the current study demonstrated that miR-125a-5p could bind to SFMBT1 and reduce the expression of SFMBT1, which was further verified by the dual-luciferase reporter gene assay. Similarly, miRNAs can bind to the 3'UTR of specific target gene mRNAs, resulting in the inhibition of mRNA degradation.³⁰ As a member of the MBT domain-containing proteins, SFMBT1 contributes to various cellular processes including the proliferation and differentiation of cells.³¹

Moreover, SFMBT1 has also been reported to be regulated by miR-20a-3p and thus mediates the TGF β 1/Survivin pathway *in vitro* to affect the proliferation and apoptosis of keratinocytes.¹⁴ Furthermore, our investigation revealed that SFMBT1 blocked the TGF β /SMAD pathway to facilitate keratinocyte proliferation and elevated the levels of IL-17A-induced cytokines. Nevertheless, activation of the TGF β /SMAD posed an inhibitory effect on IMQ-induced mouse models of psoriasis. Jiang *et al.* concluded that diminished expression of TGF β receptor-I inactivates the TGF β /SMAD pathway in the psoriatic epidermis and TGF β /SMAD/miR-486-3p axis plays an important role in the regulation of keratinocyte hyperproliferation in psoriasis.¹⁷ Notably, multifunctional TGF β has been reported to play a crucial role in the regulation of cell proliferation and differentiation and as a result it has been strongly associated with the pathogenesis of psoriasis.³² Multifunctional TGF β has been recognized as a pivotal negative regulator for keratinocyte proliferation.³³ Peculiarly, SMAD

signaling has been identified as the major pathway that restricts the differentiation of goblet cells.³⁴ SFMBT1 inhibits the expression of TGF β 1, and the extent of smad2 and smad3 phosphorylation whilst down-regulation of TGF β signaling in psoriasis could propagate the signal in cells by phosphorylation of SMAD,¹⁴ highlighting the interaction between the TGF β /SMAD pathway and keratinocyte proliferation in psoriasis. Our study provided evidence suggesting that the knockdown of EZH2 could activate the TGF β /SMAD pathway by decreasing the SFMBT1 expression which relieves psoriasis-like skin inflammation in the established mouse models. Therefore, based on the aforementioned findings, we were able to identify the effect of EZH2 on psoriasis progression promotion *in vivo*. Collectively, the key findings of our study suggest that EZH2 could potentially inactivate the TGF β /SMAD pathway by regulating the miR-125a-5p-dependent SFMBT1 during the progression of psoriatic lesions.

Certain limitations were faced during the study. The specific targeting between miR-125a-5p and SFMBT1 has been rarely explored and thus further data are required from additional studies. We also cannot exclude the involvement of other signaling pathways in the inhibition of keratinocyte proliferation post psoriasis due to the complex microenvironments. Moreover, our study was composed of a relatively small number of patients, which may cause the unicentricity of the study based in only one location. Therefore, a more comprehensive study with a large number of clinical data is required in the future to further elucidate the correlation between epigenetic factors and the progression of psoriasis with the aim of translating these findings into effective clinical therapies.

Conclusion

Altogether, the current study demonstrates that EZH2 was overexpressed while SFMBT1 and miR-125a-5p were down-regulated in psoriasis tissues and cells. EZH2 increased the levels of IL-17A-induced cytokines and promoted malignant phenotypes of HaCaT cells. Also, EZH2 reduced miR-125a-5p expression while miR-125a-5p targeted SFMBT1 to activate the TGF β /SMAD pathway. The up-regulation of miR-125a-5p abolished the effects of EZH2. Overall, EZH2 was concluded to induce the upregulation of the miR-125a-5p target SFMBT1 while acting to inhibit the TGF β /SMAD pathway, stimulating

keratinocyte proliferation and promoting IL-17A-induced cytokines, ultimately contributing to the progression of psoriasis. The current study provides fresh insight into the potential of silencing EZH2 as a means of developing a novel approach for therapeutic strategies against psoriasis.

Availability of data and materials

The authors confirm that the data supporting the findings of this study are available within the article.


Conflict of interest statement

The authors declare that there is no conflict of interest.

Funding

This research received no specific grant from any funding agency in the public, commercial, or not-for-profit sectors.

ORCID iD

Bing Wang  <https://orcid.org/0000-0001-9544-6352>

References

1. Nestle FO, Kaplan DH and Barker J. Psoriasis. *N Engl J Med* 2009; 361: 496–509.
2. Boehncke WH and Schon MP. Psoriasis. *Lancet* 2015; 386: 983–994.
3. Albanesi C, Madonna S, Gisondi P, *et al.* The interplay between keratinocytes and immune cells in the pathogenesis of psoriasis. *Front Immunol* 2018; 9: 1549.
4. Furue M, Furue K, Tsuji G, *et al.* Interleukin-17A and keratinocytes in psoriasis. *Int J Mol Sci* 2020; 21: 1275.
5. Lebwohl M. Psoriasis. *Ann Intern Med* 2018; 168: ITC49–ITC64.
6. Zhang P, Su Y, Zhao M, *et al.* Abnormal histone modifications in PBMCs from patients with psoriasis vulgaris. *Eur J Dermatol* 2011; 21: 552–557.
7. Bate-Eya LT, Gierman HJ, Ebus ME, *et al.* Enhancer of zeste homologue 2 plays an important role in neuroblastoma cell survival independent of its histone methyltransferase activity. *Eur J Cancer* 2017; 75: 63–72.
8. Liu Y, Luo W and Chen S. Comparison of gene expression profiles reveals aberrant expression of FOXO1, Aurora A/B and EZH2 in lesional psoriatic skins. *Mol Biol Rep* 2011; 38: 4219–4224.

9. Xiong J, Tu Y, Feng Z, *et al.* Epigenetics mechanisms mediate the miR-125a/BRMS1 axis to regulate invasion and metastasis in gastric cancer. *Onco Targets Ther* 2019; 12: 7513–7525.
10. Srivastava A, Meisgen F, Pasquali L, *et al.* Next-generation sequencing identifies the keratinocyte-specific miRNA signature of psoriasis. *J Invest Dermatol* 2019; 139: 2547–2550 e2512.
11. Sonkoly E, Wei T, Janson PC, *et al.* MicroRNAs: novel regulators involved in the pathogenesis of psoriasis? *PLoS One* 2007; 2: e610.
12. Delic D, Wolk K, Schmid R, *et al.* Integrated microRNA/mRNA expression profiling of the skin of psoriasis patients. *J Dermatol Sci* 2020; 97: 9–20.
13. Ali Syeda Z, Langden SSS, Munkhzul C, *et al.* Regulatory mechanism of MicroRNA expression in cancer. *Int J Mol Sci* 2020; 21: 1723.
14. Li R, Qiao M, Zhao X, *et al.* MiR-20a-3p regulates TGF-beta1/Survivin pathway to affect keratinocytes proliferation and apoptosis by targeting SFMBT1 in vitro. *Cell Signal* 2018; 49: 95–104.
15. Morikawa M, Derynck R and Miyazono K. TGF-beta and the TGF-beta family: context-dependent roles in cell and tissue physiology. *Cold Spring Harb Perspect Biol* 2016; 8: a021873
16. Hata A and Chen YG. TGF-beta signaling from receptors to smads. *Cold Spring Harb Perspect Biol* 2016; 8: a022061.
17. Jiang M, Sun Z, Dang E, *et al.* TGFbeta/SMAD/microRNA-486-3p signaling axis mediates keratin 17 expression and keratinocyte hyperproliferation in psoriasis. *J Invest Dermatol* 2017; 137: 2177–2186.
18. Rendon A and Schakel K. Psoriasis pathogenesis and treatment. *Int J Mol Sci* 2019; 20: 1475.
19. Trowbridge RM and Pittelkow MR. Epigenetics in the pathogenesis and pathophysiology of psoriasis vulgaris. *J Drugs Dermatol* 2014; 13: 111–118.
20. Rohraff DM, He Y, Farkash EA, *et al.* Inhibition of EZH2 ameliorates lupus-like disease in MRL/lpr mice. *Arthritis Rheumatol* 2019; 71: 1681–1690.
21. Liu Q, Wu DH, Han L, *et al.* Roles of microRNAs in psoriasis: immunological functions and potential biomarkers. *Exp Dermatol* 2017; 26: 359–367.
22. Pradyuth S, Rapalli VK, Gorantla S, *et al.* Insightful exploring of microRNAs in psoriasis and its targeted topical delivery. *Dermatol Ther* 2020; e14221.
23. Wu R, Zeng J, Yuan J, *et al.* MicroRNA-210 overexpression promotes psoriasis-like inflammation by inducing Th1 and Th17 cell differentiation. *J Clin Invest* 2018; 128: 2551–2568.
24. Srivastava A, Nikamo P, Lohcharoenkal W, *et al.* MicroRNA-146a suppresses IL-17-mediated skin inflammation and is genetically associated with psoriasis. *J Allergy Clin Immunol* 2017; 139: 550–561.
25. Hermann H, Runnel T, Aab A, *et al.* miR-146b Probably assists miRNA-146a in the suppression of keratinocyte proliferation and inflammatory responses in psoriasis. *J Invest Dermatol* 2017; 137: 1945–1954.
26. Vaher H, Kivihall A, Runnel T, *et al.* SERPINB2 and miR-146a/b are coordinately regulated and act in the suppression of psoriasis-associated inflammatory responses in keratinocytes. *Exp Dermatol* 2020; 29: 51–60.
27. Xu N, Brodin P, Wei T, *et al.* MiR-125b, a microRNA downregulated in psoriasis, modulates keratinocyte proliferation by targeting FGFR2. *J Invest Dermatol* 2011; 131: 1521–1529.
28. Raaby L, Langkilde A, Kjellerup RB, *et al.* Changes in mRNA expression precede changes in microRNA expression in lesional psoriatic skin during treatment with adalimumab. *Br J Dermatol* 2015; 173: 436–447.
29. Cao Q, Wang N, Ren L, *et al.* miR-125a-5p post-transcriptionally suppresses GALNT7 to inhibit proliferation and invasion in cervical cancer cells via the EGFR/PI3K/AKT pathway. *Cancer Cell Int* 2020; 20: 117.
30. Ivey KN and Srivastava D. microRNAs as developmental regulators. *Cold Spring Harb Perspect Biol* 2015; 7: a008144.
31. Lin S, Shen H, Li JL, *et al.* Proteomic and functional analyses reveal the role of chromatin reader SFMBT1 in regulating epigenetic silencing and the myogenic gene program. *J Biol Chem* 2013; 288: 6238–6247.
32. Baran W, Szepietowski JC, Mazur G, *et al.* TGF-beta(1) gene polymorphism in psoriasis vulgaris. *Cytokine* 2007; 38: 8–11.
33. Shirakata Y. Regulation of epidermal keratinocytes by growth factors. *J Dermatol Sci* 2010; 59: 73–80.
34. Feldman MB, Wood M, Lapey A, *et al.* SMAD signaling restricts mucous cell differentiation in human airway epithelium. *Am J Respir Cell Mol Biol* 2019; 61: 322–331.